International Journal of Civil Engineering and Technology (IJCIET)
Volume 9, Issue 13, December 2018, pp. 1591–1605, Article ID: IJCIET_09_13_159
Available online at http://iaeme.com/Home/issue/IJCIET?Volume=9&Issue=13
ISSN Print: 0976-6308 and ISSN Online: 0976-6316

KINETICS AND ISOTHERM MODELING OF ADSORPTION OF RHODAMINE B DYE ONTO CHITOSAN SUPPORTED ZEROVALENT IRON NANOCOMPOSITE (C-nZVI)

A. Oluwasogo Dada*
Industrial Chemistry Programme, Department of Physical Sciences, Landmark University, P.M.B.1001, Omu-Aran, Kwara State, Nigeria

A. A. Inyinbor
Industrial Chemistry Programme, Department of Physical Sciences, Landmark University, P.M.B.1001, Omu-Aran, Kwara State, Nigeria

F. A. Adekola
Department of Industrial Chemistry, University of Ilorin, P.M.B. 1515, Nigeria

E. O. Odebunmi
Department of Chemistry, University of Ilorin, P.M.B. 1515, Nigeria

O. S. Bello
Department of Pure and Applied Chemistry, Faculty of Pure and Applied Sciences, Ladoke Akintola University of Technology, Ogbomoso, Nigeria

S. Ayo-Akere
Industrial Chemistry Programme, Department of Physical Sciences, Landmark University, P.M.B.1001, Omu-Aran, Kwara State, Nigeria
*Corresponding Author's E-mail: dada.oluwasogo@lmu.edu.ng

ABSTRACT

The kinetics and isotherm modeling of adsorption of Rhodamine B (RhB) Dye onto chitosan supported zerovalent iron nanocomposite (C-nZVI) was successfully studied in a batch technique. The quantity adsorbed increased with increase in initial concentration from 49.33 mg – 242.37 mg for 200 ppm to 1000 ppm and high percentage removal efficiency (%RE) of 99.72% attained at 90 minutes contact time. Equilibrium data were analyzed by six isotherm models: Langmuir, Freundlich, Temkin, Dubinin-Kaganer-Raduskevich (DKR), Redlich-peterson and Halsey isotherm model. Equilibrium data best fitted to Freundlich isotherm supported by Halsey isotherm model. Langmuir monolayer adsorption capacity (256.41 mg/g) of C-nZVI obtained greater than most adsorbent reported for adsorption of RhB. The mean

adsorption free energy, E per molecule evaluated from DKR model was less than 8 KJmol^{-1} indicating a physisorption mechanism. The kinetic data best fitted to pseudo second-order kinetic model as validated by sum of square error (SSE) statistical model and the mechanism controlled by pore diffusion. The study revealed the great potential of C-nZVI for effective removal of RhB dye. C-nZVI is therefore recommended for civic and industrial effluents treatment.

Key words: Chitosan-Iron Nanocomposite, Rhodamine B, Adsorption, Kinetics, Isotherm modeling

Cite this Article: A. Oluwasogo Dada, A. A. Inyinbor, F. A. Adekola, E. O. Odebunmi, O. S. Bello, S. Ayo-Akere, Kinetics and Isotherm Modeling of Adsorption of Rhodamine B Dye Onto Chitosan Supported Zerovalent Iron Nanocomposite (C-nZVI), *International Journal of Civil Engineering and Technology (IJCIET)* 9(13), 2018, pp. 1591–1605.
http://iaeme.com/Home/issue/IJCIET?Volume=9&Issue=13

1. INTRODUCTION

Nanotechnology is an upcoming area in the study of Chemistry. In view of the marvelous use of nanotechnology, scientists carry out various studies in this most vital discipline. Nano-materials have been reported to be applicable in environmental remediation, catalysis, development of optical devices and medicine [1-3]. Its application is continually growing and researchers are exploring the development of novel nano-adsorbents for environmental remediation [4].

The release of dyes into the environment via anthropogenic activities has been a global concern due to some adverse effects posed on the environment. Dyes are mostly used in industries such as textile, leather, paper, plastics and cosmetics to impart colour on their final products [5-6]. The release of coloured wastewater from these industries may present an ecotoxic hazard and introduce the potential danger of bioaccumulation, which may eventually affect man and aquatics through the food chain. Wastewater containing even a minute amount of dyes can severely affect the aquatic life due to the reduction of light penetration and dissolved oxygen [7].

The application of biopolymers such as chitosan is one of the emerging adsorption methods for the removal of dyes and heavy metal ions, even at low concentrations [8]. Chitosan is a type of natural polyamino-saccharide, synthesized from the deacetylation of chitin, which is a polysaccharide consisting predominantly of unbranched chains of β-(1→4)-2-acetoamido-2-deoxy-D-glucose. Chitosan is known as an ideal natural support for enzyme immobilization because of its special characteristics such as hydrophilicity, biocompatibility, biodegradability, non-toxicity, adsorption properties, etc. [9]. Chitosan can be used as an adsorbent to remove heavy metals and dyes due to the presence of amino and hydroxyl groups, which can serve as an active site [10]. There are two important advantages of chitosan as an adsorbent: firstly, its low cost compared to commercial activated carbon; secondly, its outstanding chelation behaviour. Especially in the environmental engineering field. Chitosan and its derivative have attained a good reputation as adsorbents for the removal of various contaminants, including heavy metal ions or species, fluorides, dyes, phenol and its derivatives, and many other natural or man-made pollutants [11].

Rhodamine B is the dye under investigation in this research. It is a cationic dye commonly used in textile industry due to its good fastness to fabrics and high solubility. However, it has been reported to be carcinogenic [12-13]. Although previous researchers have investigated the removal of Rhodamine B dye and other dye types utilizing different nano-adsorbent,

BiOBr/montmorillonite composites [14], Magnetic nanocomposite [15]; NiO nanoparticles [16]; Cobalt nanoparticles-embedded magnetic ordered mesoporous carbon [17]; treated epicarp of Raphia Hookerie [18], microwave and chemically treated *Acacia nilotica* leaf [19]; activated carbon [20], rice hull-based silica supported iron catalyst [21]. However, there is no report on adsorption of Rhodamine B onto chitosan supported zerovalent iron nanoparticles (C-nZVI). There is no extensive report on the isotherm and kinetics modeling of adsorption of Rhodamine B onto C-nZVI.

There are various methods of removing dyes, and they include chemical precipitation, membrane process, ion exchange, solvent extraction, electrodialysis, and reverse osmosis [13, 22]. These methods are non-economical and have many disadvantages such as incomplete dyes removal, high reagent and energy consumption, and generation of toxic sludge or other waste products that require disposal or treatment [23]. However, adsorption has proven to be superior than other techniques because it is efficient and cost effective. Various methods have all been investigated in the removal of Rhodamine B as well as other types of dyes which are calcareous, yet to our knowledge, the adsorption of Rhodamine B dye onto chitosan supported zerovalent iron nanocomposite (C-nZVI) has not been reported. The objective of this study is to investigate the modeling of kinetics and equilibrium data vis-à-vis the kinetics, mechanism and isotherm modeling of adsorption of Rhodamine B. The kinetics was studied using pseudo-first order, pseudo-second order and intraparticle diffusion models in order to determine the rate and mechanism of adsorption process. The equilibrium data were fitted to six isotherm models: Langmuir, Freundlich, Temkin, Dubinin-Kaganer-Raduskevich (DKR), Redlich-Peterson and Halsey isotherm model. Adsorption kinetics and isotherm models were investigated to develop an insight of controlling reaction pathways (e.g., chemisorption versus physisorption), determine the mechanisms (e.g. intraparticle diffusion) of the adsorption process, predict the rate at which a target contaminant would be removed from aqueous solutions and quantify the adsorptive capacity of an adsorbent (e.g C-nZVI). The results from this study can be used to assess the efficacy of C-nZVI for dyes removal and design a waste treatment reactor for industries.

2. MATERIAL AND METHODS

2.1. Chemical Reagents

All the reagents used were of analytical grade mostly purchased from Sigma-Aldrich, USA. Sodium Borohydride ($NaBH_4$) (Sigma-Aldrich, USA) was used for the chemical reduction, other reagents used were: Absolute Ethanol (BDH), Ferric Chloride ($FeCl_3$), HNO_3, Rhodamine B Dye all purchased from Sigma-Aldrich, USA.

2.2. Synthesis of Chitosan Supported Zerovalent Iron Nanocomposite (C–nZVI)

Chitosan supported iron nanocomposite was prepared using bottom-up approach via chemical reduction. Firstly, chitosan which served as the base material and one of the precursors was prepared following a similar procedure [24]. 4 g of Chitosan was dissolved in 100 mL of 2% 2% acetic acid; stir the mixture for 4 hours using a magnetic stirrer to ensure homogeneous mixture. Thereafter, zerovalent iron nanoparticle was prepared by chemical reduction following a procedure reported by Dada *et al.*[25 – 27].

Accurately weighed 10 g of nZVI was mix with 100 mL of 4% chitosan, these were stirred thoroughly for another 4 hours with the aid of a magnetic stirrer to ensure that chitosan anchors properly into the matrix of the synthesized zerovalent iron nanoscale particles to form C–nZVI nanocomposite. The C–nZVI was separated using vacuum filtration with 0.45µm Millipore filter paper. Equation of reaction is as stated below:

$$C + 4Fe^{3+} + 3BH_4^- + 9H_2O \rightarrow C\text{–}4Fe\downarrow + 3H_2BO_3^- + 12H^+ + 6H_2\uparrow \quad (1)$$

Where C represents Chitosan

2.3. Preparation of stock solution of Rhodamine B.

0.01 M Rhodamine B was dissolved in de-ionized water and made up to mark in 1000 mL standard flask. Lower concentrations of the absorbate used for adsorption studies were prepared using serial dilution. Working concentrations from 200 – 1000 ppm were used for the study.

2.4 Batch Adsorption Experiment

Effect of initial concentration and contact time were studied in a batch technique at pH 3 and ambient temperature. 100 mg of the C-nZVI was added to 25 cm^3 of RhodamineB (RhB) dye of 100 – 1000 ppm in a 50 cm^3 conical flask. The mixture was agitated intermittently on the regulated mechanical shaker for 3 hrs and the residual concentration of RhB was determined in triplicate using Biochrom Libra PCB 1500 Double Beam UV –VIS spectrophotometer. Effect of contact time was studied from 10 – 120 minutes at optimum conditions. Adsorption capacities and the removal efficiency were obtained using Eqs.2 and 3 respectively [28]:

$$q_e = \frac{(C_o - C_e)V}{W} \tag{2}$$

$$\% \ E = \frac{C_o - C_e}{C_o} \times 100 \tag{3}$$

The equilibrium data were fitted into ten isotherm models and the kinetic data were analyzed using pseudo first-order, pseudo second-order and intraparticle diffusion models.

3. THEORY

3.1. Adsorption Isotherm Modeling

The interaction between RhB and the C-nZVI can be well described using isotherm models. In this study ten isotherm models were utilized in describing the equilibrium data vis-à-vis Langmuir, Freundlich, Temkin, DKR, Redlich Peterson and Halsey. Presented in Table 1 are the linear equations and corresponding parameters plotted in fitting the isotherm models. The evaluated parameters were determined from the slope and intercept of their linear plots as portrayed in Table 1

3.1.1. Langmuir isotherm model

This model assumes a surface monolayer and homogeneous adsorption that occurred on finite number of identical active sites with uniform energies of adsorption. Each site can accommodate one adsorbate and there is no interaction between neighboring adsorbed molecules or atoms [25, 29]. The Langmuir parameters q_{max} (maximum monolayer coverage capacity, $mg.g^{-1}$) and K_L (Langmuir isotherm constant, $L.mg^{-1}$) were determined from the slope and intercept of the linear plot. The essential feature of Langmuir isotherm may be expressed in terms of the R_L, which is referred to as separation factor or dimensionless constant as seen in Eq. 16 [27]:

$$R_L = \frac{1}{1 + K_L C_o} \tag{16}$$

3.1.2. Freundlich Isotherm Model

The Freundlich adsorption isotherm (Table 1, Eq. 5) gives an expression encompassing the surface heterogeneity and the exponential distribution of active sites and their energies. The

Freundlich isotherm constants, K_f and n indicating the sorption capacity and intensity respectively are parameters characteristic of the adsorbent-adsorbate system.

3.1.3. Temkin Isotherm

The Temkin isotherm model (Table 1, Eq. 6) describes the adsorbent-adsorbate interaction as having the heat of adsorption of all molecules in the layer decreasing linearly with the surface coverage [23, 30]. The parameter $\boldsymbol{b_T}$ is the Temkin isotherm constant related to the heat of sorption and A_T is the Temkin isotherm equilibrium binding constant (Lg^{-1}).

3.1.4. Dubinin-Kaganer-Raduskevich (DKR) isotherm model

DKR isotherm model (Table 1, Eq. 7) gives insight into the physical and chemical nature of the adsorption process. From the linear equation in Table 1, $A_{D\text{-}R}$ is the DRK isotherm constant (mol^2/kJ^2) related to free sorption energy and Q_d is the theoretical isotherm saturation capacity (mg/g).The mechanism of the process was judged from the mean sorption free energy, E per molecule of RhB adsorbate computed by the relationship in Eq. 17 [13, 25, 31]:

$$E = -\left[\frac{1}{\sqrt{2A_{D-R}}}\right] \tag{17}$$

3.1.5. Redlich-Peterson (R-P) Isotherm model

The R-P isotherm model (Table 1, Eq. 8) combines both elements from the Langmuir and Freundlich isotherm models as an empirical isotherm incorporating three parameters. The mechanism of adsorption is a mix hence does not obey monolayer adsorption [32-33]. When β=1, it reduces to Langmuir equation with B=b (Langmuir adsorption constant (Lmg^{-1}) which is related to the energy of adsorption. $A_{R\text{-}P} = bq_{max}$ where q_{max} is Langmuir maximum adsorption capacity of the adsorbent (mgg^{-1}).

3.1.6. Halsey isotherm model

The Halsey isotherm model (Table 1, Eq. 9) is used to evaluate the multilayer adsorption at a relatively large distance from the surface. [34-35].

Table 1 Different adsorption isotherms [3, 4, 23, 33, 36]

S/N	Isotherms models	Linear Equations	Equations	Plot	Evaluated Parameters
1	Langmuir	$\frac{C_e}{q_e} = \frac{1}{K_L q_{\max}} + \frac{C_e}{q_{\max}}$	4	$\frac{C_e}{q_e}$ vs C_e	$q_{\max}$, K_L
2	Freundlich	$\ell ogq_e = \ell ogK_f + \frac{1}{n}\ell ogC_e$	5	ℓogq_e vs ℓogC_e	K_f, $\frac{1}{n}$, and n
3	Temkin	$q_e = \frac{RT}{b_T}\ln A_T + \frac{RT}{b_T}\ln Ce$	6	q_e vs ℓnC_e	A_T , b_T , β
4	DKR	$\ell nq_e = \ell nq_m - A_{D-R}\varepsilon^2$	7	ℓnq_e vs ε^2	q_m , A_{D-R}
5	Redlich-Peterson	$\ln\left(\frac{C_e}{q_e}\right) = \beta\ln C_e - \ln A_{R-P}$	8	$\ln\left(\frac{C_e}{e}\right)$ $vs\ln C_e$	β , A_{R-P}
8	Halsey	$\ell nq_e = \left[\left(\frac{1}{n_H}\right)\ell nK_H\right] - \left(\frac{1}{n_H}\right)\ell nC_e$	9	ℓnq_e vs ℓnC_e	$\frac{1}{n_H}$, n_H, K_H

3.2. Kinetics Modeling and Statistical Validity

The kinetic data were subjected to pseudo first-order, pseudo second-order and intraparticle diffusion models in order to determine the rate and mechanism of the adsorption process.

3.2.1. Pseudo-First Order Kinetics Model.

The linear form of pseudo first–order equation is generally expressed as:

$$Log(q_e - q_t) = Log\ q_e - \frac{k_1 t}{2.303} \tag{10}$$

Where q_e is the quantity of RhB adsorbed at equilibrium per unit weight of the C-nZVI nano-adsorbent (mg/g), q_t is the amount of RhB adsorbed at any time (mg/g) and k_1 is the pseudo first-order rate constant (min^{-1}). Pseudo first-order parameters were determined from the plot of $log(q_e - q_t)$ against t [37]

3.2.2. Pseudo-Second Order Kinetics Model

The linear form of Pseudo second-order rate expression is given by the expression:

$$\frac{t}{q_t} = \frac{1}{k_2 q_e^2} + \frac{1}{q_e} t \tag{11}$$

When t tends to 0, h_2 is defined as:

$$h_2 = k_2 q_e^2 \tag{12}$$

Substituting h_2 into Eq.20, it becomes:

$$\frac{t}{q_t} = \frac{1}{h_2} + \frac{1}{q_e} t \tag{13}$$

Where h_2 is the initial adsorption rate for pseudo second-order. (The pseudo second – order parameters determined from the plot of $\mathbf{t/q_t}$ against t [38].

3.2.3. Intraparticle Diffusivibility

The intraparticle diffusion equation is expressed as:

$$q_t = k_{id} t^{0.5} + C \tag{14}$$

Where k_{id} is the intraparticle diffusion rate constant ($mg.g^{-1}min^{0.5}$) and C is the intercept indicating the thickness of C-nZVI. The q_t is the amount of solute adsorbed per unit weight of adsorbent per time, (mg/g), and $t^{0.5}$ is the half adsorption time [3, 4, 39].

3.2.4. Validity of the Kinetics Data

The suitability, agreement and best fit among the kinetic models were judged using the statistical tools such as regression coefficient (R^2), sum of square error (SSE) Sum of square error (SSE) is the mostly used by researchers. The mathematical expression is given in Eq. 23 [25, 26, 36, 39]:

$$SSE = \sum_{i=1}^{n} \left(q_{e,cal} - q_{e,\exp}\right)^2 \tag{15}$$

3. RESULTS AND DISCUSSION

3.1. Bulk Density, Moisture Content, Point of Zero Charge and FTIR Characterization of (C-nZVI)

The synthesized Chitosan supported zerovalent iron nanocomposite was characterized by point of zero charge (PZC), moisture content, and bulk density (Physico-chemical

characterization) and FTIR (spectroscopic characterization). The point of zero charge (PZC) is defined as the pH at which that surface area has a net neutral charge [25, 40]. The PZC of C-nZVI found to be 4. This was significance and suitable for the adsorption of Rhodamine B at a pH below the point of zero charge. Moisture content 7.2 and bulk density 0.731 gcm^{-3} were indication of good equilibration of the C-nZVI with the adsorbate (RhB) thus preventing floatation [41]. The FTIR analysis of C-nZVI was done using SHIMADZU FTIR model IR8400s Spectrophotometer. This was done prior to the adsorption to determine the functional groups, molecular environment of the adsorbents and examine the possible sites of interaction of Rhodamine B with C-nZVI. The FTIR spectrum of chitosan supported iron nanoparticles prior to adsorption is shown in the Fig. 1, the spectra reveals the characteristic band at 3433.29 cm^{-1} indicating the presence of –OH functional group on the surface of the chitosan supported zero-valent iron. The vibration band at the region of 1641cm^{-1} indicates the presence of C=O, the presence of iron nanoparticle is observed at the region of 698-478 cm^{-1} [42].

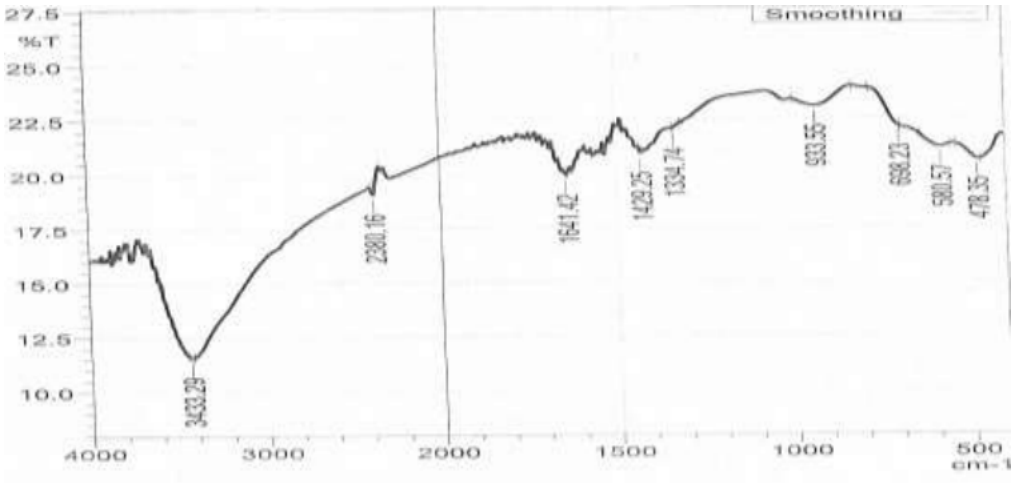

Figure 1: FTIR spectrum for C-nZVI

3.2. Effect of Initial Concentration on Adsorption of Rhodamine B onto Chitosan supported Zerovalent Iron Nanocomposite (C-nZVI)

Concentration plays a key role as a driving force to overcome the mass transfer resistance between the Rhodamine B solution and C-nZVI. Fig 2 shows the removal efficiency of RhB at different initial concentrations from 200 ppm to 1000 ppm. It was observed that the adsorption capacity and removal efficiency increased with increase in concentration is due to the concentration gradient developed at solid-liquid interface. At higher concentration of RhB, the active sites of C-nZVI were bombarded by more of the dye molecules as the process continued until a saturated point was reached. The quantity adsorbed increased with increase in initial concentration due to the availability of the active sites from 49.33 mg – 242.37 mg for 200 ppm to 1000 ppm. More so, removal efficiency increased from 98.65% to 99.72% until equilibrium was reached between 800 – 1000 ppm. Advantageously, removal efficiency as high as 96% was attained at highest concentration (1000 ppm) indicating the effectiveness of C-nZVI in RhB adsorption. This finding is in support with the report in the literature [3, 4, 43]

3.3. Effect of Contact time on Adsorption of Rhodamine B onto Chitosan supported Zerovalent Iron Nanocomposite (C-nZVI)

Contact time is also an important factor in all transfer phenomena such as adsorption. Presented in Figure 3 is the contact time at various initial concentrations. The experimental conditions are well stated below the plot. It was observed that rate of reaction was rapid from 10 min and equilibrium was attained at 30 min indicating a fast adsorption enhanced by this novel chitosan supported zerovalent iron nanocomposite (C-nZVI) [42, 43]. This is one of the advantages of nanoadsorbents. A steady state approximation sets in and a quasi-equilibrium situation attained all through from 30 minutes to 120 minutes.

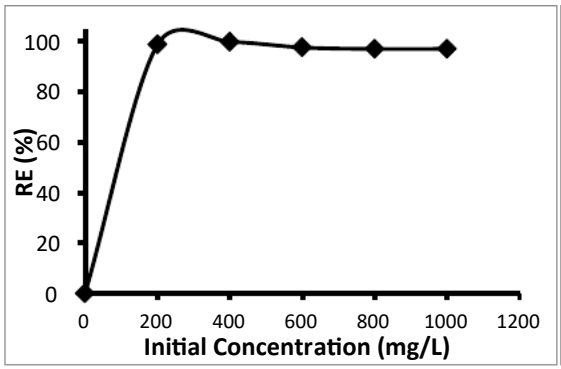

Figure 2: Effect of Initial Conc.
Experimental Conditions: C-nZVI Dose=100 mg, Tempt= 25°C, pH = 3, Time = 90 minutes, Stirring Speed = 120rpm

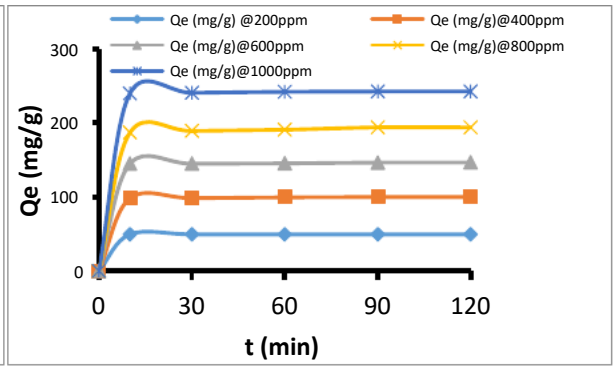

Figure 3: Effect of Contact Time at Various Initial Conc
Experimental Conditions: C-nZVI Dose = 100 mg
T= 25 °C, pH = 3, Stirring Speed = 120 rpm

3.4. Kinetics and Mechanism modeling of Adsorption of Rhodamine B onto C-nZVI

Presented in Figures 4 – 6 are linear plots of pseudo first-order, pseudo second-order and intraparticle diffusion models at various concentrations. Their evaluated are well presented in Table 2. From the regression coefficient (R^2) point of view, it was clearly observed that the kinetic experimental data gave the best fits with the pseudo-second order kinetic model having a correlation co-efficient of $R^2>0.99$ at all concentrations. Also, the close agreement between the values of experimental and calculated quantity adsorbed, $q_{e,\ exp}$ and $q_{e,\ cal}$ respectively corroborated that kinetic data were best described by pseudo second-order model. This was validated by the lower values of sum of square error (SSE) at all concentrations as observed in Table 2. The lower the values of SSE, the better the kinetic model in describing the kinetic process [25 – 28, 44]. Higher values of SSE observed in pseudo first–order (Fig. 4) from 2,343.77 – 55, 774.66 is an indication of poor fitting of pseudo first-order model.

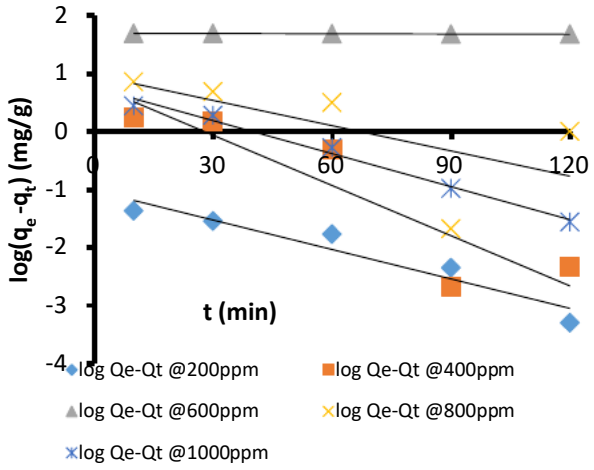

Figure 4 Pseudo first-order kinetic model for model adsorption of RhB onto C-nZVI

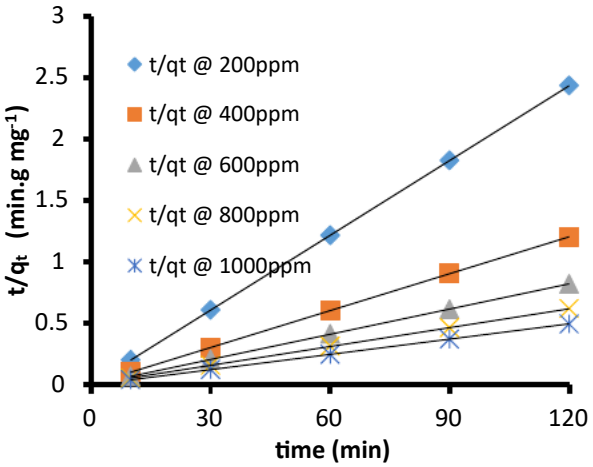

Figure 5: Pseudo second order kinetic for adsorption of RhB onto C–nZVI

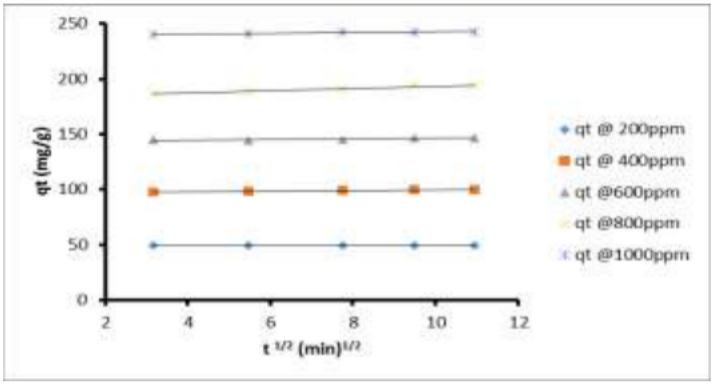

Figure 6: Intraparticle diffusion model plot for adsorption of RhB onto C-nZVI

The determination of the adsorption rate controlling step enhances understanding of the adsorption mechanism. In order to determine the mechanism, kinetic data were tested with Weber's intraparticle diffusion model. From the evaluated parameters in Table 2, close values and agreement among experimental, calculated quantity adsorbed, $q_{e,\,exp}$ and $q_{e,\,cal}$, and the intercept, C (boundary layer), higher regression coefficient (R^2>0.92) and lower values of SSE confirmed that the mechanism was governed and controlled by pore diffusion. The intercept (C) which is the thickness of the surface gives information about the contribution of the surface adsorption in the rate determining step. The larger the intercept, the greater the contribution of the pore to adsorption [3]. However, since the intraparticle diffusion plots (Figure 6) did not pass through the origin, it therefore indicated that intraparticle diffusion is not the only rate determining step [23, 44].

Table 2: Parameters of different kinetic and mechanism models of RhB dye adsorption onto C-nZVI

Pseudo First-order	**200 ppm**	**400 ppm**	**600 ppm**	**800 ppm**	**1000 ppm**
k_1	0.0389	0.0665	0.00046	0.0333	0.0437
q_e,exp	49.33	99.24	145.222	190.66	241.88
$q_e cal$	0.0957	6.3547	49.6935	9.4015	5.7134
R^2	0.9174	0.8251	0.9212	0.3923	0.9875
SSE	2,343.77	8,627.67	9,125.69	32,854.6	55,774.7
Pseudo Second-order	**200 ppm**	**400 ppm**	**600 ppm**	**800 ppm**	**1000 ppm**
k_2	1.36	0.02	0.02	$6.7x10^{-3}$	0.02
q_e,exp	49.33	99.24	145.222	190.66	241.88
$q_e cal$	49.26	100	147.05	196.07	243.9

R^2	1	1	1	0.9999	1
h_2	3309.49	196.97	421.77	243.55	1170.11
SSE	$4.9x10^{-3}$	0.57	3.34	29.26	4.08
Intraparticle Diffusion	***200 ppm***	**400 ppm**	**600 ppm**	**800 ppm**	**1000 ppm**
q_e *exp*	49.33	99.24	145.222	190.66	241.88
q_e, *cal*	*49.51*	*122.52*	*179.05*	*375.48*	*325.52*
$k_{ip}(mg/g/min^{0.5})$	0.0044	0.2546	0.2419	0.9905	0.358
C	49.295	97.122	143.65	183.49	238.75
R^2	0.9863	0.943	0.8486	0.9635	0.9534
SSE	0.033162	541.889	1144.042	3,4157.83	6,995.708

3.5. Adsorption Isotherm Models for the Uptake of Rhodamine B using Chitosan Supported Iron Nanocomposite (C-nZVI)

The interaction between RhB and the C-nZVI was well described using isotherm models. In this research, six different isotherm models were fitted to the equilibrium data vis-à-vis Langmuir, Freundlich, Temkin, Dubinin-Kaganer-Radushkevich (D–R), Redlich-Peterson, and Halsey isotherm models and their corresponding equations as presented in Table 1. Linear plots of these isotherm models are depicted in Figure 7(A-J). Specifically, the linear least-squares method and the linearly transformed equations have been widely applied to correlate sorption data.

Judging from the correlation coefficient, equilibrium data were fitted to Langmuir isotherm model with R^2 = 0.926. R_L Value indicates the adsorption nature to either unfavourable or unfavourable. It is unfavourable if R_L >1, linear if R_L=1, favourable if 0< R_L <1 and irreversible if R_L= 0. The value of the separation factor, R_L (Fig 8) ranging from $3x10^{-2}$ - $6.14x10^{-3}$which is less than unity is an indication of a favourably adsorption [3, 23, 45].

However, based on higher R^2 values observed in Freundlich (Fig 7B), Redlich Peterson (Figure 7E) and Halsey (Fig. 7F), the adsorption process is physisorption in nature hence a multilayer adsorption. Both k_f and n are Freundlich constant and adsorption intensity respectively. The value of $1/n_f$ is less that unity indicating high heterogeneity of the C-nZVI nature, value of n (2.39) lying between one and ten is an indication of normal and favourable adsorption [27, 46].

From Temkin isotherm model (Fig 7C), low value of heat of adsorption is an indications of physisorption mechanism and endothermic nature of the adsorption process [28]. Dubinin-Kaganer-Raduskevich (DKR) isotherm model (Fig 7D) gives insight into the physical and chemical nature of the adsorption process. Since the magnitude of E (free energy of transfer of one solute from infinity to the surface of C-nZVI) is less than 8 kJ mol^{-1} (Table 3), the electrostatic forces coupled with pore diffusion as a result of mass transport played a substantial role in adsorption process supporting physisorption mechanism. This finding corroborated the assertion in Freundlich and Temkin isotherm models [34, 43].

Freundlich isotherm adequately described the equilibrium data than Langmuir suggesting a multilayer adsorption process and this is supported by the results from Halsey isotherm models parameters (Table 3) [47-48]

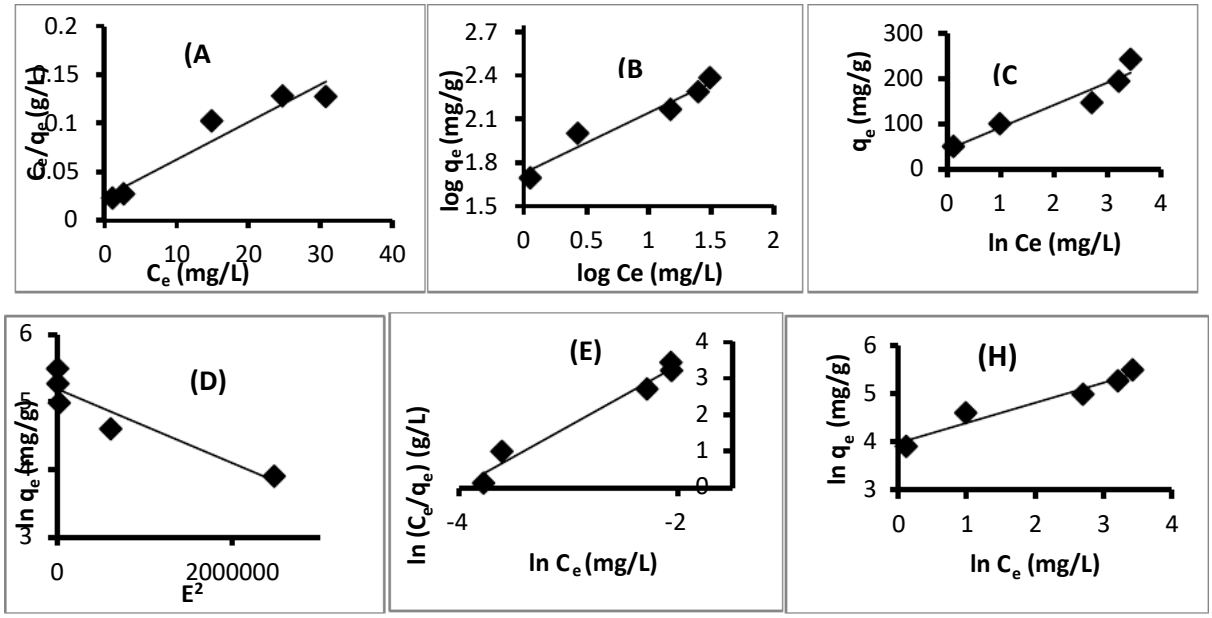

Figures 7 (A-F): Linear plots of: (A) Langmuir (B) Freundlich (C) Temkin (D) DKR (E) Redlich Peterson (F) Halsey Isotherm model

Table 3: Isotherm models parameters for adsorption of RhB onto C-nZVI

Langmuir		**Freundlich**		**Temkin**	
q_{max} (mgg^{-1})	256.41	k_f	53.27	b_T($J\ mol^{-1}$)	179.77
K_L (Lmg^{-1})	0.1618	$1/n_f$	0.4177	β(Lg^{-1})	5×10^{-7}
R_L	3×10^{-2} - 6.14×10^{-3}	n_f	2.3941	A_T (Lg^{-1})	1
R^2	0.926	R^2	0.9458	R^2	0.871
DKR		Redlich Peterson		Halsey	
q_d	179.77	A_{R-P}	1.242×10^{-3}	$1/n_H$	-0.4176
A_{DKR}	5×10^{-7}	B_{R-P}	1.668	n_H	-2.3946
E(KJ/mol)	1	q_{max}	7.45×10^{-4}	K_H	7.34×10^{-5}
R^2	0.871	R^2	0.9714	R^2	0.9458

4. CONCLUSIONS

Chitosan supported zerovalent iron nanocomposite (C-nZVI) was successfully prepared using a chemical reduction method in a single pot system. The result from the bulk density, moisture content and point of zero charge indicated that C-nZVI was suitable in the uptake of Rhodamine B. They were characterized by Fourier Transform infra-red spectroscopy to determine the functional group present. The point of zero- charge (PZC) revealed that these adsorbents are suitable for the removal of cationic dyes from waste water bodies. It also further explains the properties of the adsorbents having a strong affinity for the removal of Rhodamine B dye from aqueous solution; their effectiveness depends largely on their composition. The adsorption capacities were found to depend on the quantity of adsorbents, contact time and initial concentration. The kinetic data were best described by pseudo-second order and the mechanism was governed by intraparticle diffusion. The equilibrium data were best fitted to Freundlich isotherm model supported by Halsey isotherm models indication a multilayer adsorption on heterogeneous surface of C-nZVI. The adsorption process was physisorption as confirmed by the energy values estimated from Dubinin-Kaganer-Radushkevich model which was found to be less than 8kJ mol^{-1}. Results obtained from this study showed that C-nZVI is a potential, effective and efficient adsorbent in the uptake of

Rhodamine dye B (RhB) from aqueous solution. C-nZVI is thereby recommended for treatment of civic waste.

ACKNOWLEDGMENT

Dada, Adewumi Oluwasogo and co-authors appreciate the Management of Landmark University for the financial support and enabling environment provided for result oriented research.

REFERENCES

[1] Dada, A. O., Adekola, F. A., Adeyemi, O, S., Bello, M. O., Adetunji, C. O., and Awakan, O. J. (2018). Book Chapter Titled: Exploring the Effect of Operational Factors and Characterization Imperative to the Synthesis of Silver Nanoparticles. In: Book Title: Silver Nanoparticles - fabrication, characterization and applications. Chapter 9, pg 165 – 184. Doi.org/10.5772/intechopen.76947 ISBN 978-953-51-6035-9

[2] Dada, A. O., Inyinbor, A. A., Idu, I. E., Bello, O. M., Oluyori, A. P., Adelani-Akande, T. A., Okunola, A. A., Dada, O. Effect of operational parameters, characterization and antibacterial studies of green synthesis of Silver Nanoparticles, using Tithonia diversifolia. *PeerJ* (2018) DOI 10.7717/peerj.5865 (in-press)

[3] Dada AO, Adekola FA, Odebunmi EO. Liquid phase scavenging of Cd (II) and Cu (II) ions onto novel nanoscale zerovalent manganese (nZVMn): Equilibrium, kinetic and thermo-dynamic studies. Environmental Nanotechnology, Monitoring & Management. 8 (2017)[a], 63-72. http://dx.doi.org/10.1016/j.enmm.2017.05.001

[4] Dada, A. O., Adekola, F. A., Odebunmi, E. O. Kinetics and equilibrium models for Sorption of Cu(II) onto a Novel Manganese Nano-adsorbent. *Journal of Dispersion Science and Technology* 37(1), (2016) , 119 – 133

[5] Ciardelli G, Corsi L, Marcucci M Membrane separation for waste water reuse in the textile industry. *Res Conserv Recy*, 31, (2000), 189–197.

[6] Inyinbor, A. A., Adekola, F. A., and Olatunji, G. A. EDTA Modified *Irvingia gabonensis*: An Efficient Bioresource Material for the Removal of Rhodamine B. *Pak. J. Anal. Environ. Chem.* 16(2), (2015)38 – 47

[7] Robinson, T., MacMullan, G., Marchant, R., Nigam, P. Remediation of dyes textile effluent: A critical review on current treatment technologies with a proposed alternative. *Bioresource Technology, 77* (2001), 247 – 255

[8] Crini.G. Non-conventional low cost adsorbents for dye removal. Bioresource Technology, 97, (2006), 1061–1085.

[9] Perju, M. M. and Dragan, E. S. Removal of azo dyes from aqueous solutions using chitosan based composite hydrogels. *Ion Exchange Letters*, 3 (2010): 7-11

[10] Zhang J., Zhang, Y., Li, R., Pan Q. Synthesis, characterization and adsorption properties of a novel chitosan derivative.*Indian Journal of Chemical Technology*, 19 (2012), 161 – 166.

[11] Copello, G. J., Varela, F., Vivot, R. M., Diaz, L. E. Immobilized chitosan as biosorbent for the removal of Cd(II), Cr(III) and Cr(VI) from aqueous solutions, *Bioresour Technol*. 99, (2008), 6538 – 6544.

[12] Inyinbor, A. A., Adekola, F. A. and Olatunji, G. A. Kinetic and thermodynamic modeling of liquid phase adsorption of Rhodamine B dye onto Raphia hookerie fruit epicarp; Water Resources and Industry, Vol 15 (2016), pg 14 –27

[13] Dada, A. O., Olalekan, A. P., Olatunya, A. M., Dada, O. Langmuir, Freundlich, Temkin and Dubinin–Radushkevich Isotherms Studies of Equilibrium Sorption of Zn^{2+} onto Phosphoric Acid Modified Rice Husk . *Journal of Applied Chemistry, 3(1), (2012)[a], 38 – 45*

[14] Xu, C., Wu, H., Gu, F. L. Efficient adsorption and photocatalytic degradation of Rhodamine Bunder visible light irradiation over BiOBr/montmorillonitecomposites ,*Journal of Hazardous Materials* 275 (2014), 185–192

[15] Singha, K. P., Gupta, S., Singha, A. K and Sinha, S. Experimental design and response surface modeling for optimization of Rhodamine B removal from water by magnetic nanocomposite, *Chemical Engineering Journal* 165 (2010), 151–160

[16] Motaharia, F., Mozdianfard, M. R., Salavati-Niasari, M. Synthesis and adsorption studies of NiO nanoparticles in the presence of H_2acacen ligand for removing Rhodamine B in wastewater treatment. *Process Safety and Environmental Protection*, 93, (2015), 282–292

[17] Tanga, L., Caia, Y., Yanga, G., Yuanyuan, L, Zenga, G, Zhoua, Y, Lia, S., Wanga, J., Zhanga, S., Fanga, Y., He, Y. Cobalt nanoparticles-embedded magnetic ordered mesoporouscarbon for highly effective adsorption of Rhodamine B. *Applied Surface Science* 314 (2014), 746–753

[18] Inyinbor, A. A., Adekola, F. A. & Olatunji, G. A. Adsorption of Rhodamine B from Aqueous Solution Using Treated Epicarp of RaphiaHookerie. *Covenant Journal of Physical and Life Sciences*, 2(2), (2014), 84 – 101

[19] Santhi, T., Prasad, A. L., Manonmani, S. A comparative study of microwave and chemically treated Acacia nilotica leaf as an ecofriendly adsorbent for the removal of rhodamine B dye from aqueous solution.*Arabian Journal of Chemistry,*7, (2014),: 494–503

[20] Li, L., Liu, S., Zhu, T. (2010). Application of activated carbon derived from scrap tires for adsorption of Rhodamine B. *Journal of Environmental Sciences*, 22(8) (2010) 1273 –1280

[21] Gan, P. P., Li, S. F. Y. Efficient removal of Rhodamine B using a rice hull-based silica supported iron catalyst by Fenton-like process, *Chemical Engineering Journal* 229 (2013), 351–363

[22] Dada, A. O., Inyinbor, A. A., Oluyori, A. P. Comparative Adsorption of Dyes onto Activated Carbon Prepared From Maize Stems And Sugar Cane Stems. *Journal of Applied Chemistry,* 2(3) (2012)[b], 38 – 43

[23] Dada, A.O.,Ojediran, J.O., and Olalekan, A.P., (2013). Sorption of Pb^{2+} from Aqueous Solution unto Modified Rice Husk: Isotherms Studies. *Advances in Physical Chemistry,* Volume 2013, http://dx.doi.org/10.1155/2013 /842425 pp 1-6

[24] Vakili, M., Rafatullah, M., Salamatinia, B., Abdullah, A. Z., Ibrahim, M. H., Tan, K. B., Gholami, Z., Amouzgar, P. Application of chitosan and its derivatives as adsorbents for dye removal from water and wastewater: A Review. *Carbohydr. Polym.* 113, (2014), 115–130

[25] Dada, A. O., Adekola, F. A. and Odebunmi, E. O. Kinetics, Mechanism, Isotherm and Thermodynamic Studies of Liquid Phase Adsorption of Pb^{2+} onto Wood Activated Carbon Supported Zerovalent Iron (WAC-ZVI) Nanocomposite. *Cogent Chemistry Journal,* 3(2017)[b]: 1351653, pg 1- 20. DOI: http://doi.org/10.1080/23312009.2017.1351653

[26] Dada, A. O., Adekola, F. A. and Odebunmi, E. O. Novel zerovalent manganese for removal of copper ions: Synthesis, Characterization and Adsorption studies. *Applied water Science*, 7 (2017)[c],1409–1427 Doi: 10.1007/s13201-015-0360-5

[27] Dada, A. O., Latona, D. F., Ojediran, O. J. Adsorption of Cu(II) onto Bamboo Supported Manganese (BS-Mn) Nanocomposite: Effect of Operational Parameters, Kinetics,

Isotherms, and Thermodynamic Studies. *Journal of Applied Sciences and Environmental Management (JASEM)* Vol. 20 (2), (2016), 409 – 422

[28] Dada, A. O., Adekola, F. A., Odebunmi, E. O. Isotherm, kinetics and thermodynamics studies of sorption of Cu^{2+} onto novel zerovalent iron nanoparticles. *Covenant Journal of Physical and Life Sciences*, 2(1), (2014), 24 -53.

[29] Langmuir, I. 1918. "The adsorption of gases on plane surfaces of glass, mica and platinum". *Journal of the American Chemical Society*, 40: (1918), 1361–14 03.

[30] Temkin, M. I., Pyzhev, V., 1940. Kinetic of Ammonia Synthesis on Promoted Iron Catalysts. Acta Physiochim. URSS 12, (1940), 327-356.

[31] Dubinin, M. M. 1960. The potential theory of adsorption of gases and vapors for adsorbents with energetically non-uniform surface. Chem. Rev. 60, (1960), 235–266.

[32] Brouers, F., Al-Musawi, T. J., "On the optimal use of isotherm models for the characterization of biosorption of lead on algae," *Journal of Molecular Liquids*, 212, (2015),pp.46–51,2015.

[33] Ayawei, N., Ebelegi, A. N., Wankasi, D. Modelling and Interpretation of Adsorption Isotherms. Hindawi Journal of Chemistry, Volume 2017, Article ID 3039817, https://doi.org/10.1155/2017/3039817

[34] Song, C., Wu, S., Cheng, M., Tao, P., Shao, M., and Gao, G.. Adsorption Studies of Coconut Shell Carbons Prepared by KOH Activation for Removal of Lead (II) from Aqueous Solutions. *Sustainability*, 6, (2014), 86-98

[35] Bhatt, R. R. and Shah, B. A. "Sorption studies of heavy metal ions by salicylic acid formaldehyde–catechol terpoly-meric resin: Isotherm, kinetic and thermodynamics". *Arabian Journal of Chemistry* , 8(3), (2015), 414 – 426.

[36] Foo, K. Y. and Hameed, B. H (2010). Review: Insights into the modeling of adsorption isotherm systems. *Chemical Engineering Journal,* 156 (2010), 2 – 10.

[37] Ho, Y. S., Chiu, W-T., Hsu, C-S., Huang, C-T. (2004). Sorption of lead ions from aqueous solution using tree fern as a sorbent. *Hydrometallurgy*, 73 (2004): 55 – 61

[38] Ahmad, M. A., Puad, N. A. A., Bello, O. S. Kinetic, equilibrium and thermodynamic studies of synthetic dye removal using pomegranate peel activated carbon prepared by microwave-induced KOH activation. *Water Resources and Industry,* 6 (2014), 18 – 35.

[39] Boparai, H.K., Meera, J., and Dennis, M. O. (2011. "Kinetics and thermodynamics of Cadmium ion removal by adsorption onto nano zerovalent iron particles". *Journal of Hazardous Material* 186: 458 – 465

[40] Jaafar MZ, Nasir AM, Hamid MF (2013) Point of zero charge for sandstone and carbonate rocks by streaming potential. Int J Pet Geosci Eng 1(2):82–90

[41] Kumar, Y. K., Muralidhara, H. B., Nayaka, Y. A., Balasubramanyam, J., Hanumanthappa, H. Hierarchically assembled mesoporous ZnO nanorods for the removal of lead and cadmium by using differential pulse anodic stripping voltammetric method. *Powder Technology* 239 (2013): 208 –216

[42] Venkatraman, B.R., Gayathri, U., Elavarasi, S., and Arivoli, S. (2012). Removal of Rhodamine B dye from aqueous solution using the acid activated Cynodondactylon carbon, Der Chemica Sinica, 2012, 3(1):99-113

[43] Olakunle, M. O., Inyinbor, A.A., Dada, A.O. & Bello, O.S., (2017) Combating dye pollution using cocoa pod husks: A sustainable approach. International Journal of Sustainable Engineering, 11 (1) (2017), Pages 4-15, http://dx.doi.org/10.1080/19397038.2017.1393023

[44] Bello, O. S, Ahmad , M. A, Semire, B. (2014). Scavenging malachite green dye from aqueous solutions using pomelo (Citrusgrandis) peels: kinetic, equilibrium and thermodynamic studies. *Desalination and Water Treat ment* 2014)oi: 10.1080/19443994.201 4.940387

[45] Hao, Y-M; Chen, M; Hu, Z-B. Effective removal of Cu (II) ions from aqueous solution by amino-functionalized magnetic nanoparticles, J Hazard Maters. 184 (2010): 392–399

[46] Peng, X., Lam, F. L. Y., Wang, Y., Liu, Z.,. Adsorption behavior and mechanisms of Ciprofloxacin from aqueous solution by ordered mesoporous carbon and bamboo-based carbon. *J. Colloid and Interface Sci,* (2015) doi: http://dx.doi.org/10.1016/ j.jcis.2015.08.050

[47] Xu, C., Wu, H., Gu, F. L. Efficient adsorption and photocatalytic degradation of RhodamineBunder visible light irradiation over BiOBr/montmorillonitecomposites ,*Journal of Hazardous Materials* 275 (2014), 185–192

[48] Wang, J., Zheng, S., Shao, Y., Liu, J. 2010. "Amino-functionalized Fe_3O_4–SiO_2 core–shell magnetic nanomaterial as a novel adsorbent for aqueous heavy metals removal". *Journal of Colloid and Interface Science*, 349: 293–299.